Green's function approach to the thermodynamic properties of the anisotropic Kondo necklace model

H. Rezania and A. Langari*
Physics Department, Sharif University of Technology, Tehran 11155-9161, Iran

P. Thalmeier
Max Planck Institute for Chemical Physics of Solids, 01187 Dresden, Germany

(Received 12 November 2008; revised manuscript received 8 January 2009; published 3 March 2009)

We have studied the two-dimensional anisotropic Kondo necklace model with antiferromagnetic (AF) Kondo coupling $J_\perp$ and exchange coupling between "itinerant" spins J on the square lattice. The bond operator formalism is used to transform the spin model to a hard-core bosonic gas. We have used the Green's function approach to obtain the temperature dependence of spin excitation spectrum (triplet gap). We have also found the temperature dependence of the specific heat and the local spin-correlation function between localized and itinerant spins for various Kondo couplings $J_\perp/J$ and anisotropies in both coupling strengths. Furthermore we studied the temperature dependence of the structure factor for localized spins which is determined by effective interactions via itinerant spins. For low temperature and close to the quantum critical point we have obtained an analytical formula for temperature dependence of the energy gap and specific heat. Finally we compared our results with those of previous mean-field treatments.

DOI: 10.1103/PhysRevB.79.094401 PACS number(s): 75.10.Jm, 75.30.Mb, 75.30.Kz, 75.40.Mg

I. INTRODUCTION

Heavy fermion compounds[1–3] have received continued attention, in particular their quantum critical behavior and related superconducting properties. In these intermetallic compounds, strongly correlated electrons in f orbitals are hybridized with conduction electrons resulting in a strongly enhanced quasiparticle density of states at the Fermi level.[3] This is signified by a large value for Pauli susceptibility and specific heat at low temperature.

The generic model which describes these properties is the Kondo lattice model (KLM) with the Hamiltonian

$$H_{\mathrm{KL}} = t\sum_{\langle ij\rangle,\boldsymbol{\tau}} (c^{\dagger}_{i,\boldsymbol{\tau}} c_{j,\boldsymbol{\tau}} + \mathrm{h.c.}) + J_\perp \sum_i \boldsymbol{\tau}_i \mathbf{S}_i. \tag{1}$$

The first part represents the kinetic energy of conduction electrons $c^{\dagger}_{i,\tau}$ with nearest-neighbor hopping t. The second part is the Kondo term where $\boldsymbol{\tau}_i$ is the spin of conduction electrons and $\mathbf{S}_i$ is the spin of localized moments. Sufficiently above a characteristic temperature, T^*, localized electrons behave as a collection of independent free moments. Below T^*, the competition between Kondo-singlet coupling and induced RKKY interactions may either lead to a paramagnetic state with fully screened moments $[J_\perp/t > (J_\perp/t)_c]$ or a long-range antiferromagnetic (AF) ordered state with reduced moments $(J_\perp/t < (J_\perp/t)_c)$. In the former case a Landau Fermi-liquid state with large effective mass appears below a coherence temperature $T_{\mathrm{FL}} < T^*$, in the latter AF order is stabilized below the Néel temperature $T_N > T^*$. Changing the control parameter $(J_\perp/t)$ leads to a quantum phase transition between these states at a "quantum critical point" (QCP) given by $(J_\perp/t)_c$. Around the QCP there is a V-shaped region (quantum critical region) in the phase diagram where non-Fermi-liquid behavior in the thermodynamic and transport properties is observed.[2,4–6]

Numerical methods including quantum Monte Carlo (QMC) simulation,[7] density-matrix renormalization-group (DMRG) method[8] have been used to investigate the thermodynamic properties of the KLM in one dimension (1D) and two dimensions (2D). Finite temperature Lanczos method (exact diagonalization method) for finite 2D clusters for the KLM (Refs. 9 and 10) has also been used and temperature dependence of specific heat, local Kondo screening and intersite spin correlations have been obtained.

In the one-dimensional case[11] the KLM model can be mapped by Jordan-Wigner transformation to a pure spin model. Instead of a kinetic term in H_{KL} one has a XY-type nearest-neighbor spin interaction for the "itinerant" electrons. This procedure is not strictly possible in 2D or three dimensions (3D). But we can consider a KLM with correlated conduction band by adding a Coulomb repulsion of conduction electrons with strength U_c to suppress charge fluctuations. This model has been treated within dynamical mean-field theory approach[12] (DMFT) where the spatial correlations are neglected but the dynamics of interactions is included. In this approach, at relatively high-temperature conduction electrons are almost decoupled from the localized electrons. With decreasing temperature, the particle-hole symmetric model for half filling exhibits insulating behavior with a gap in the one-particle spectral function whose size increases with U_c. In addition, using a cumulant expansion for the partition function, the charge and spin susceptibility and specific heat for KLM with correlated conduction band have been calculated.[13] In the limit of very large U_c and half filled conduction band, the kinetic term and strong Coulomb repulsion are replaced by a spin exchange $J=4t^2/U_c$ in the insulating state. Strictly speaking the resulting effective spin model is only appropriate for Kondo insulators where charge degrees of freedom are frozen but one may expect that it also describes the low energy spin dynamics of more metallic Kondo systems. The generalized "Kondo necklace model" (KNM) obtained in this way is given by[14]

 ©2009 The American Physical Society

$$H = J\sum_{\langle i,j\rangle}(\tau_i^x\tau_j^x + \tau_i^y\tau_j^y + \delta\tau_i^z\tau_j^z) + J_\perp\sum_i(\tau_i^xS_i^x + \tau_i^yS_i^y + \Delta\tau_i^zS_i^z). \quad (2)$$

In the present work we will study the finite temperature properties in the anisotropic KNM for the first time. We have implemented the bond operator formalism[15,16] which has been used before within mean-field approximation[17,18] to determine the quantum critical phase diagram. It should be noticed that the mean-field approach fails to predict the quantum phase transition in the anisotropic one-dimensional model.[19] In a more advanced treatment the KNM spin Hamiltonian in Eq. (2) is mapped to hard-core bosonic gas composed of four types of bosonic particles: three components of a triplet and a singlet boson. The former are spin excitations in the original model. In a previous work,[20] we obtained the energy gap of triplet excitation spectrum versus $J_\perp/J$ and its dependence on the anisotropy parameters (Δ,δ). For each set of anisotropy parameters we found the quantum critical point where excitation energy vanishes. Here we will investigate the temperature dependence for the excitation energy and calculate internal energy and specific heat. Furthermore we obtain local spin-correlation function and the static structure factor from one and two-particle Green's functions, respectively.

Previously, thermodynamic quantum critical properties of the anisotropic Kondo necklace model have been studied within mean-field approach[21,22] where the equation for the lines separating quantum critical and paramagnetic or AF regimes was derived analytically. Similarly expressions for specific heat in the Kondo-singlet phase and quantum critical region were found. We will compare these analytical results with our numerical results from the hard-core boson Green's function approach. Results for the related bilayer *isotropic* Heisenberg model have been previously obtained by the same method and the specific heat around the QCP was investigated by using QMC simulations.[23]

II. BOSONIC HAMILTONIAN AND FINITE TEMPERATURE GREEN'S FUNCTION

The Hamiltonian in Eq. (2) is written in terms of bond operators[15,16] as defined in Eqs. (3)–(13) of Ref. 20. The bond operator transformation[15,16] is applied in the anisotropic Kondo necklace model of Eq. (2). In the momentum space, the noninteracting part of the Hamiltonian has the form[20]

$$H_2 = \sum_{k,\alpha}A_{k,\alpha}t_{k,\alpha}^\dagger t_{k,\alpha} + \sum_{k,\alpha}\frac{B_k}{2}(t_{k,\alpha}^\dagger t_{-k,\alpha}^\dagger + \text{h.c.}), \quad (3)$$

where $t_{k,\alpha}^\dagger$ and $t_{k,\alpha}$ $(\alpha=x,y,z)$ are the creation and annihilation of a triplet as a bond operator.[20] The coefficients in the above equation are

$$A_{k,z} = J_\perp + \delta J\xi_k, \quad A_{k,x(y)} = \frac{J_\perp}{2}(1+\Delta) + J\xi_k,$$

$$B_{k,z} = \delta J\xi_k, \quad B_{k,x(y)} = J\xi_k,$$

$$\xi_k = [\cos k_x + \cos k_y]/2. \quad (4)$$

The other parts of the Hamiltonian which describe triplet boson interactions are represented by H_3 and H_4. The explicit representation of H_3 and H_4 is given by Eqs. (7) and (8) in Ref. 20. Both H_3 and H_4 are of higher order in triplet operators which lead to small corrections in the spectrum.[20] Therefore the effect of H_3 and H_4 is considered on a mean-field level. The dominant contribution to the renormalization of the spectrum comes from the constraint where only one of the triplet states can be excited on every site (the boson hard-core condition) $t_{\alpha i}^\dagger t_{\beta i}^\dagger = 0$, which can be taken into account by introducing an infinite on-site repulsion between the bosons. The boson hard-core condition in the momentum space is given by

$$H_U = U\sum_{k,k',q,\alpha,\beta}t_{\alpha k+q}^\dagger t_{\beta k'-q}^\dagger t_{\beta k'}t_{\alpha k}, \quad (5)$$

where k,k',q are wave vectors and α,β are the x,y,z components. The Bogoliubov transformation,

$$\tilde{t}_{k,\alpha} = u_{k,\alpha}t_{k,\alpha} + v_{k,\alpha}t_{-k,\alpha}^\dagger, \quad (6)$$

diagonalizes the Hamiltonian [Eq. (3)] to

$$H_2 = \sum_{k,\alpha}\omega_{k,\alpha}\tilde{t}_{k,\alpha}^\dagger\tilde{t}_{k,\alpha}, \quad (7)$$

where the triplet-mode frequencies $\omega_\alpha(k)(\alpha=x,y,z)$ in the single-particle picture are given by

$$\omega_{k,\alpha}^2 = A_{k,\alpha}^2 - B_{k,\alpha}^2, \quad (8)$$

and the Bogoliubov coefficients are

$$u_{k,\alpha}^2(v_{k,\alpha}^2) = (-)\frac{1}{2} + \frac{A_{k,\alpha}}{2\omega_{k,\alpha}}. \quad (9)$$

In the previous work,[20] we have considered the low-density approximation for bosonic gas at zero temperature as a starting point. A note is in order here that the generalization of this method to finite temperature is valid if our consideration is restricted to low temperatures; $T<J_\perp,J$.

The noninteracting normal Matsubara Green's functions is $g_{n,\alpha}(k,\tau) = -\langle T_\tau[t_{k,\alpha}(\tau)t_{k,\alpha}^\dagger(0)]\rangle$ and the anomalous Matsubara bosonic Green's function is $g_{a,\alpha}(k,\tau) = -\langle[T_\tau t_{k,\alpha}^\dagger(\tau)t_{-k,\alpha}^\dagger(0)]\rangle$. Using the Fourier transformation defined in the Ref. 24 the normal and anomalous Green's functions may be written as

$$g_{n,\alpha}(k,i\omega_n) = \frac{u_{k,\alpha}^2}{i\omega_n - \omega_{k,\alpha}} - \frac{v_{k,\alpha}^2}{i\omega_n + \omega_{k,\alpha}}, \quad (10)$$

$$g_{a,\alpha}(k,i\omega_n) = \frac{u_{k,\alpha}v_{k,\alpha}}{i\omega_n - \omega_{k,\alpha}} - \frac{u_{k,\alpha}v_{k,\alpha}}{i\omega_n + \omega_{k,\alpha}}. \quad (11)$$

The interacting Green's functions are obtained from Dyson's equation for each Green's function (anomalous or normal). The perturbation expansion and the implementation of Wick's theorem (contracting pairs of operators) are possible only in the Matsubara representation.[25] The simple poles of the retarded Green's functions are the one-particle excitations of the model. It has been demonstrated[24] that a simple analytical continuation in the Fourier space can transform Matsubara Green's function to the retarded Green's function

which is correct for both interacting and noninteracting case. The retarded Green's function is

$$G_{\alpha}^{\mathrm{Ret}}(k,t) = -i\theta(t)\langle[t_{k,\alpha}(t), t_{k,\alpha}^{\dagger}(0)]\rangle, \tag{12}$$

where the analytic continuation is obtained by the following transformation

$$G_{\alpha}^{\mathrm{Ret}}(k,\omega) = g_{\alpha}(k, i\omega_n \rightarrow \omega + i\delta). \tag{13}$$

The spectral function which its peaks are the one-particle excitations is related to the retarded Green's function by

$$R_{\alpha}(k,\omega) = -2\ \mathrm{Im}[G_{\alpha}^{\mathrm{Ret}}(k,\omega)]. \tag{14}$$

The perturbative expansion for the interacting Green's function in the Matsubara notation[24] (for each polarization component of the triplet bosons) is

$$\bar{g}(k,i\omega_n) = \overline{g^0}(k,i\omega_n)[1 - \overline{g^0}(k,i\omega_n)\bar{\Sigma}(k,i\omega_n)]^{-1}. \tag{15}$$

Similar to Ref. 20, the interacting Green's function $[\bar{g}(k,i\omega_n)]$ and the self-energy $[\bar{\Sigma}(k,\omega)]$ are 2×2 matrices

$$\bar{g}(k,i\omega_n) = \begin{pmatrix} G_n(k,i\omega_n) & G_a(k,i\omega_n) \\ G_a(k,i\omega_n) & G_n(-k,-i\omega_n) \end{pmatrix},$$
$$\bar{\Sigma}(k,i\omega_n) = \begin{pmatrix} \Sigma_n(k,i\omega_n) & \Sigma_a(k,i\omega_n) \\ \Sigma_a(k,i\omega_n) & \Sigma_n(-k,-i\omega_n) \end{pmatrix}. \tag{16}$$

The combination of Eqs. (10), (11), (15), and (16) gives the following relation for the interacting normal Green's function

$$g_{n,\alpha}(k,i\omega_n) = \frac{i\omega_n + A_{k,\alpha} + \Sigma_{n,\alpha}(-k,-i\omega_n)}{[i\omega_n + A_{k,\alpha} + \Sigma_{n,\alpha}(k,-i\omega_n)][i\omega_n - A_{k,\alpha} - \Sigma_{n,\alpha}(k,i\omega_n)] + [B_k + \Sigma_{a,\alpha}(k,i\omega_n)]^2}. \tag{17}$$

To get the low energy (single particle) excitation spectrum, the retarded form of Eq. (17) should be separated into the bosonic single-particle excitation (collective modes of the original spin model) and incoherent background. After expanding the retarded self-energy in the low energy limit, the single-particle part of Green's function can be written in the following form:

$$G_{n,\alpha}^{\mathrm{sp}}(k,\omega) = \frac{Z_{k,\alpha}U_{k,\alpha}^2}{\omega - \Omega_{k,\alpha} + i\eta} - \frac{Z_{k,\alpha}V_{k,\alpha}^2}{\omega + \Omega_{k,\alpha} + i\eta}, \tag{18}$$

where the renormalized triplet spectrum and the renormalized single-particle weight constants are given by

$$\Omega_{k,\alpha} = Z_{k,\alpha}\sqrt{\{A_{k,\alpha} + \mathrm{Re}[\Sigma_{n,\alpha}^{\mathrm{Ret}}(k,0)]\}^2 - \{B_{k,\alpha} + \mathrm{Re}[\Sigma_{a,\alpha}^{\mathrm{Ret}}(k,0)]\}^2},$$

$$Z_{k,\alpha}^{-1} = 1 - \left(\frac{\partial\ \mathrm{Re}(\Sigma_{n,\alpha}^{\mathrm{Ret}})}{\partial\omega}\right)_{\omega=0},$$

$$U_{k,\alpha}^2(V_{k,\alpha}^2) = (-)\frac{1}{2} + \frac{Z_{k,\alpha}\{A_{k,\alpha} + \mathrm{Re}[\Sigma_{n,\alpha}^{\mathrm{Ret}}(k,0)]\}}{2\Omega_{k,\alpha}}. \tag{19}$$

The renormalized weight constant is the residue of the single-particle pole of the Green's function.

III. EFFECT OF INTERACTING PARTS OF HAMILTONIAN ON THE BOSONIC EXCITATIONS

The density of the triplet excitations is obtained from normal Matsubara Green's functions:

$$\rho_{\alpha,i} = \langle t_{\alpha i}^{\dagger} t_{\alpha i}\rangle = \frac{1}{N}\sum_{k,\alpha}\{[1 + 2n_B(\omega_{k,\alpha})]v_{k,\alpha}^2 + n_B(\omega_{k,\alpha})\}, \tag{20}$$

where $n_B(\omega)$ is the Bose-Einstein distribution and N is the number of the unit cells in the square lattice. Since the Hamiltonian H_U in Eq. (5) is short ranged and U is large, the Brueckner approach (ladder diagram summation)[25] can be applied for low temperature and low-density limit of the triplet boson gas. Generally, it is similar to the approach implemented in Ref. 26, however, technically it is more demanding due to the effect of anisotropies (δ,Δ) and finite temperature. The interacting normal Green's function is obtained by imposing the hard-core boson repulsion. First, we introduce the scattering amplitude $\Gamma_{\alpha\beta,\gamma\delta}(p_1,p_2;p_3,p_4)$ of triplet bosons where $p_i=[\mathbf{p},(ip_n)]_i$, $p_n=\frac{2n\pi}{\beta}$. The scattering amplitude or self-energy for the two-particle Green's function depends on the total energy and momentum of the incoming particles. The nonretarded and local character of U leads to $\Gamma_{\alpha\beta,\gamma\delta}=\Gamma\delta_{\alpha\gamma}\delta_{\beta\delta}$. The basic approximation made in the derivation of $\Gamma(K)$ is that we neglect all anomalous scattering vertices, which are present in the theory due to the existence of anomalous Green's functions. According to the Feynman rules in momentum space at nonzero temperature and after taking the limit $U\rightarrow\infty$ we can write for the scattering amplitude (in Fig. 1 of Ref. 20),

$$\Gamma_{\alpha\beta,\alpha\beta}(\mathbf{K},i\omega_n) = \left(\frac{1}{\beta(2\pi)^3}\sum_{Q_m}\int d^3Q g_{\alpha\alpha}^0(Q)g_{\beta\beta}^0(K-Q)\right)^{-1}. \tag{21}$$

where, $p_1+p_2=p_3+p_4\equiv K=(\mathbf{K},i\omega_n)$. To find the solution self-consistently, we should replace (the noninteracting) $g^0\rightarrow g$ (by the interacting Green's function) in Eq. (21). We use the Lehmann representation or fluctuation-dissipation theorem[24] which relates the Matsubara Green's function (for both interacting and noninteracting Green's function) to the

spectral function,

$$g_\alpha(\mathbf{k}, i\omega_n) = \int_{-\infty}^{\infty} \frac{d\omega}{2\pi} \frac{R_\alpha(\mathbf{k},\omega)}{i\omega_n - \omega},$$

$$R_\alpha(\mathbf{k},\omega) = -2\,\mathrm{Im}[G^{\mathrm{Ret}}(\mathbf{k},\omega)]. \tag{22}$$

The scattering amplitude Γ in Eq. (21) is obtained as (see Appendix A),

$$\Gamma_{\alpha\beta,\alpha\beta}(\mathbf{K}, i\omega_n) = -\left(\frac{1}{(2\pi)^3}\int d^3Q\left[u^2_{\mathbf{Q},\alpha}u^2_{\mathbf{K-Q},\beta}\left(\frac{n_B(\omega_{\mathbf{Q},\alpha})}{i\omega_n - \omega_{\mathbf{Q},\alpha} - \omega_{\mathbf{K-Q},\beta}} - \frac{n_B(-\omega_{\mathbf{K-Q},\beta})}{i\omega_n - \omega_{\mathbf{K-Q},\beta} - \omega_{\mathbf{Q},\alpha}}\right)\right.\right.$$
$$- u^2_{\mathbf{Q},\alpha}v^2_{\mathbf{K-Q},\beta}\left(\frac{n_B(\omega_{\mathbf{Q},\alpha})}{i\omega_n - \omega_{\mathbf{Q},\alpha} + \omega_{\mathbf{K-Q},\beta}} - \frac{n_B(\omega_{\mathbf{K-Q},\beta})}{i\omega_n + \omega_{\mathbf{K-Q},\beta} - \omega_{\mathbf{Q},\alpha}}\right) - v^2_{\mathbf{Q},\alpha}u^2_{\mathbf{K-Q},\beta}\left(\frac{n_B(-\omega_{\mathbf{Q},\alpha})}{i\omega_n + \omega_{\mathbf{Q},\alpha} - \omega_{\mathbf{K-Q},\beta}}\right.$$
$$\left.\left.\left. - \frac{n_B(-\omega_{\mathbf{K-Q},\beta})}{i\omega_n - \omega_{\mathbf{K-Q},\beta} + \omega_{\mathbf{Q},\alpha}}\right) + v^2_{\mathbf{Q},\alpha}v^2_{\mathbf{K-Q},\beta}\left(\frac{n_B(-\omega_{\mathbf{Q},\alpha})}{i\omega_n + \omega_{\mathbf{Q},\alpha} + \omega_{\mathbf{K-Q},\beta}} - \frac{n_B(\omega_{\mathbf{K-Q},\beta})}{i\omega_n + \omega_{\mathbf{K-Q},\beta} + \omega_{\mathbf{Q},\alpha}}\right)\right]\right)^{-1}. \tag{23}$$

The normal self-energy is then obtained by using the vertex function of Eq. (23),

$$\Sigma^U_{\alpha\alpha}(\mathbf{k}, i\omega_n) = -\sum_{\gamma\beta}\sum_{p_m}\int \frac{d^3p}{\beta(2\pi)^3}\Gamma_{\alpha\beta,\gamma\delta}(p,k;k,p)g_{\gamma\beta}(\mathbf{p}, ip_m) - \sum_{\beta\delta}\sum_{p_m}\int_{-\infty}^{\infty}\frac{d^3p}{\beta(2\pi)^3}\Gamma_{\alpha\beta,\gamma\delta}(p,k;p,k)g_{\delta\beta}(p). \tag{24}$$

Using the result of Eq. (22) for spectral densities, the x component of the self-energy is given by

$$\Sigma^U_{xx}(\mathbf{k}, i\omega_n) = \frac{3}{(2\pi)^3}\int d^3p[u^2_{\mathbf{p},x}n_B(\omega_{\mathbf{p},x})\Gamma_{xx,xx}(\mathbf{p}+\mathbf{k}, \omega_{\mathbf{p},x} + i\omega_n) - v^2_{\mathbf{p},x}n_B(-\omega_{\mathbf{p},x})\Gamma_{xx,xx}(\mathbf{p}+\mathbf{k}, -\omega_{\mathbf{p},x} + i\omega_n)]$$
$$+ \frac{1}{(2\pi)^3}\int d^3p[u^2_{\mathbf{p},z}n_B(\omega_{\mathbf{p},z})\Gamma_{xz,xz}(\mathbf{p}+\mathbf{k}, \omega_{\mathbf{p},z} + i\omega_n) - v^2_{\mathbf{p},z}n_B(-\omega_{\mathbf{p},z})\Gamma_{xz,xz}(\mathbf{p}+\mathbf{k}, -\omega_{\mathbf{p},z} + i\omega_n)]. \tag{25}$$

We can simply obtain the retarded self-energy by analytic continuation ($i\omega_n \to \omega + i\eta$) of Eq. (25). The analytical continuation in Γ [Eq. (23)] creates a term of $i\eta$ in the denominator of each fraction. According to Cauchy's theorem only the principal part $[\frac{1}{x+i\eta} = Pr.\frac{1}{x} - i\pi\delta(x)]$ will contribute, and the imaginary part of the self-energy vanishes. The frequency (ω) is very small and the model is treated close to the quantum critical point (but not at this point) which leads the values of $\omega_{\mathbf{Q},\alpha}$ be different from ω except at the critical point. Consequently, for low energy limit, the spectral function for the triplet bosons has sharp peaks in the excitation spectrum [Eqs. (18) and (19)]. Generally, this spectrum is a function of temperature.

H_3 is much smaller than H_U, thus we can consider the effect of H_3 on the excitation spectrum in the second-order perturbation theory. After algebraic calculation for Dyson's series and using the Feynman rules for nonzero temperature[25] we can obtain the second-order self-energy due to H_3. The formula for the self-energy contribution (either normal or anomalous) is quite lengthy and has been given in Appendix B.

The contribution of H_4 on the final results is very small because it is composed of quartic terms in the triplet operators. It is therefore treated in mean-field approximation. This is equivalent to take only the one-loop diagrams into account (first order in J). On the mean-field level we have $O_1O_2 = \langle O_1\rangle O_2 + \langle O_2\rangle O_1 - \langle O_2\rangle\langle O_1\rangle$ where each O_1 and O_2 is a pair of boson triplet operators. We can write for each pair of operators,

$$\langle t^\dagger_{i,\alpha}t_{j,\alpha}\rangle = -\frac{1}{\beta N}\sum_n\sum_k e^{ik.(R_j-R_i)-i\omega_n 0^+}G^{\alpha\alpha}_n(k, i\omega_n)$$
$$= \frac{1}{N}\sum_k e^{ik.(R_j-R_i)}\{[1+2n_B(\omega_{k,\alpha})]v^2_{k,\alpha} + n_B(\omega_{k,\alpha})\},$$
$$\langle t^\dagger_{i,\alpha}t^\dagger_{j,\alpha}\rangle = \frac{1}{N}\sum_k e^{ik.(R_j-R_i)}u_{k,\alpha}v_{k,\alpha}[1+2n_B(\omega_{k,\alpha})]. \tag{26}$$

Thus, the effect of H_4 is to renormalize A and B coefficients according to the following relations,

$$A_{k,z} \to A_{k,z} + 2J\xi_k\frac{1}{N}\sum_q\{[1+2n_B(\omega_{q,z})]v^2_{q,z} + n_B(\omega_{q,z})\}\xi_q,$$

$$B_{k,z} \to B_{k,z} - 2J\xi_k\frac{1}{N}\sum_q u_{q,x}v_{q,x}[1+2n_B(\omega_{q,x})]\xi_q,$$

$$A_{k,(x,y)} \to A_{k,(x,y)} + J\xi_k\frac{1}{N}\sum_q\{\delta v^2_{q,(x,y)}[1+2n_B(\omega_{q,x})]$$
$$+ v^2_{q,z}[1+2n_B(\omega_{q,z})] + n_B(\omega_{q,z}) + n_B(\omega_{q,x})\}\xi_q,$$

$$B_{k,(x,y)} \to B_{k,(x,y)} - J\xi_k\frac{1}{N}\sum_q\{\delta u_{q,(x,y)}v_{q,(x,y)}[1+n_B(\omega_{q,x})]$$
$$+ u_{q,z}v_{q,z}[1+n_B(\omega_{q,z})]\}\xi_q. \tag{27}$$

The renormalized coefficients [Eq. (27)] will be considered to calculate the normal and anomalous self-energy which are independent of energy (nonretarded in time representation).

IV. INTERNAL ENERGY

First, we obtain the internal energy (E) in terms of one-particle Green's function by the equation of motion. Then, the specific heat is obtained from the temperature derivative of internal energy, $C_V=\frac{\partial E}{\partial T}$. The Hamiltonian $H=H_0+H_1$ is divided into the noninteracting (H_0) and interacting (H_1) parts, where $H_0=H_{J_\perp}$, $H_1=H_J+H_U+H_3+H_4$. Here, the exchange interaction between the local and itinerant electron spin is decoupled into two parts according to $H_2=H_{J_\perp}+H_J$. In this respect, we can define the thermal average of the interacting part to the single-particle Green's function. To do so, we multiply the equation of motion for the annihilation operator ($\frac{d}{d\tau}t_{i,\alpha}=[H,t_{i,\alpha}]$) from the left side by a creation operator

$$\begin{aligned}
&\lim_{\tau_1\to\tau^+}\frac{1}{2}\sum_{i,\alpha}\left\{t^\dagger_{i,\alpha}(\tau_1)\frac{d}{d\tau}t_{i,\alpha}(\tau)+\frac{d}{d\tau_1}[t^\dagger_{i,\alpha}(\tau_1)]t_{i,\alpha}(\tau)\right\}\\
&\quad+\sum_{i,\alpha=x,y}t^\dagger_{i,\alpha}\left[\frac{J_\perp(1+\Delta)}{2}\right]t_{i,\alpha}+\sum_i t^\dagger_{i,z}J_\perp t_{i,z}\\
&=-2(H_U+H_4)-H_J-\frac{3}{2}H_3\\
&=-\left[2(H_U+H_4+H_3+H_J)-n_s\frac{\partial(H_U+H_3+H_J)}{\partial n_s}\right]. \qquad (28)
\end{aligned}$$

In the above equation $n_s=\langle s\rangle$, where s is the singlet operator. We can neglect $\frac{\partial}{\partial s^2}\langle H_1\rangle$ in Eq. (28) based on the fact that $s=1$. After writing the left-hand side of Eq. (28) in terms of normal Green's functions, ensemble average of interacting parts of Hamiltonian is written as

$$\begin{aligned}
\langle H_U+H_3+H_4+H_J\rangle&=\frac{N}{2\beta}\int\frac{d^2k}{(2\pi)^2}\sum_n e^{i\omega_n 0^+}\\
&\times\left(\sum_{\alpha=x,y}\frac{J_\perp(1+\Delta)}{2}G^n_\alpha(k,i\omega_n)+J_\perp G^n_z(k,i\omega_n)\right). \qquad (29)
\end{aligned}$$

Adding the ensemble average of $H_0=H_{J_\perp}$ to Eq. (29) and after using the Lehmann representation and summing over Matsubara frequencies, we finally obtain the thermal average of the Hamiltonian (internal energy) as

$$\begin{aligned}
E=\frac{N}{2}\int\frac{d^2k}{(2\pi)^2}&\left(\sum_{\alpha=x,y}\frac{J_\perp(1+\Delta)}{2}[Z_{\mathbf{k},\alpha}U^2_{\mathbf{k},\alpha}n_B(\Omega_{\mathbf{k},\alpha})\right.\\
&-Z_{\mathbf{k},\alpha}V^2_{\mathbf{k},\alpha}n_B(-\Omega_{\mathbf{k},\alpha})]+J_\perp[Z_{\mathbf{k},z}U^2_{\mathbf{k},z}n_B(\Omega_{\mathbf{k},z})\\
&\left.-Z_{\mathbf{k},z}V^2_{\mathbf{k},z}n_B(-\Omega_{\mathbf{k},z})]\right), \qquad (30)
\end{aligned}$$

where N is the number of unit cells.

V. ANALYTICAL CALCULATION OF TEMPERATURE-DEPENDENT ENERGY GAP AND SPECIFIC HEAT

In the vicinity of the antiferromagnetic wave vector ($|p-q_0|\ll 1$) where $q_0=(\pi,\pi)$ and close to the quantum critical point, the low-temperature excitation spectrum (the x component for anisotropic case) can be written

$$\omega_{p,x}=\sqrt{E_g^2(T)+c_x^2(p-q_0)^2}, \qquad (31)$$

where c_x is the spin-wave velocity.[23,26–28] The latter is the slope of dispersion of the x-component excitations close to q_0 and will be calculated numerically. To find the energy gap we should consider the excitation energy at the wave vector q_0

$$E_g^2(T)=[A^2_{q_0,x}(T)-B^2_{q_0,x}(T)]Z_{q_0,x}, \qquad (32)$$

where $A_{q_0,x}, B_{q_0,x}$ are coefficients in the one-particle part of the Hamiltonian which has to be renormalized by self-energies of the interacting parts. Now, we consider the variation with temperature, keeping J and $J_\perp$ fixed close to the quantum critical point.

$$\begin{aligned}
A_{q_0,x}(T)&=A_{q_0,x}(T=0)+\partial\Sigma^U_{n,x}(q_0)+\partial\Sigma^3_{n,x}(q_0)+\partial\Sigma^4_{n,x}(q_0),\\
B^c_{q_0,x}(T)&=B^c_{q_0,x}(T=0)+\partial\Sigma^3_{a,x}(q_0)+\partial\Sigma^4_{a,x}(q_0), \qquad (33)
\end{aligned}$$

where ∂X means the variation of X with respect to the temperature. The identity $A^c_{q_0,x}(T=0)=-B^c_{q_0,x}(T=0)$ holds at zero temperature. If we substitute Eq. (33) into Eq. (32) and neglect terms quadratic in E_g the variation of $A^c_{q_0,x}(T=0)$ and $B^c_{q_0,x}(T=0)$ must vanish. We now have to obtain the variation of each of the terms present in Eq. (33). In the first step, we calculate the variation of the self-energy related to H_U which is given by

$$\begin{aligned}
\partial\Sigma^U_x(\pi,\pi)=3\int\frac{d^2p}{(2\pi)^2}\,&\partial[(1+n_B(\Omega_{p,x}))v^2_{p,x}\Gamma_{xx,xx}\\
&\times(p+q_0,-\omega_{q,x})+n_B(\Omega_{p,x})u^2_{p,x}\Gamma_{xx,xx}\\
&\times(p+q_0,\omega_{p,x})], \qquad (34)
\end{aligned}$$

where we have assumed $\partial v^2_{p,z}=0$. Indeed for $0\le\delta<1$ the z component of the spectrum has a finite gap when the x component becomes gapless at the quantum critical point. To implement Eq. (31) we can change the variable p in Eq. (34) to q by $p-q_0\to q$ where q is the distance from the antiferromagnetic wave vector (q_0) and $q\sim\frac{E_g(T)}{c}\ll 1$. The x component of the vertex function for small q can be written as $\Gamma_{xx,xx}(q,-\omega_{q,x})\approx\Gamma^c_{xx,xx}(0)$. Therefore, Eq. (34) is reduced to

$$\begin{aligned}
\partial\Sigma^U_x(\pi,\pi)=3\int\frac{d^2q}{(2\pi)^2}\,&\partial\{[1+2n_B(\Omega_{q,x})]v^2_{q,x}\\
&+n_B(\Omega_{q,x})\}\Gamma^c_{xx,xx}(0). \qquad (35)
\end{aligned}$$

Integrating over q gives the variation of self-energy as

$$\partial\Sigma_x^U(\pi,\pi) = -\frac{3\Gamma^c_{xx,xx}(0)A^c_{q_0,x}Z^c_{q_0}}{4\pi c_x^2}\int_{E_g(0)}^{E_g(T)}\left(1+\frac{2}{e^{E_g(T)/T}-1}\right)dE_g. \tag{36}$$

Similar relations to Eq. (36) also exist for $\partial\Sigma^3_{n,x}(\pi,\pi)$, $\partial\Sigma^4_{n,x}(\pi,\pi)$. The true excitation at finite temperature is given by minimizing Eq. (32) which is equivalent to put the summation of all variations to zero. It finally leads to

$$\frac{E_g(T)}{T} = \frac{E_g(T=0)}{T} + 2\int_{E_g(T)/T}^{\infty}\frac{dy}{e^y-1}. \tag{37}$$

After a simple integration of Eq. (37) we obtain the analytic solution

$$E_g(T) = 2T\sinh^{-1}(e^{y/2}/2) \equiv Tf(y), \tag{38}$$

where $y=E_g(T=0)/T$. To find an analytical form for the specific heat, we use the energy variation $\partial E=\Sigma\Omega_{k,\alpha}\partial n_B(\Omega_{k,\alpha})$, in analogy to the Landau theory of Fermi liquids. Using Eqs. (32) and (38), the specific heat is obtained for low temperatures ($T\ll J,J_\perp$) and close to the quantum critical point[23]

$$C_v = \frac{2}{3}C_V^0\phi\left(\frac{E_g(T=0)}{T}\right)T^2, \tag{39}$$

where $C_V^0 \equiv \frac{3\zeta(3)}{2\pi c_x^2}$ is the specific heat for gapless boson gas with linear dispersion $\omega=c_xk$ and ϕ is given by

$$\phi\left(y\equiv\frac{E_g(T=0)}{T}\right) = \frac{1}{2\zeta(3)}\int_{f(y)}^{\infty}\frac{dy_1y_1e^{y_1}}{(e^{y_1}-1)^2}\left(y_1^2-f^2(y)+yf(y)\frac{df(y)}{dy}\right). \tag{40}$$

At the quantum critical point $y\to 0$ then $\phi(y)$ is a constant. The contribution of the z component excitation of triplets is negligible in comparison with the x component. Because of the anisotropy, the energy gap of z component is greater than the energy gap of the x component and according to the quadratic exponential function of energy gap in the denominator of the Eq. (40), we can approximately neglect the contribution of the z component in the specific heat.

VI. SPIN CORRELATIONS AND STATIC STRUCTURE FACTOR FOR LOCALIZED SPINS

The spin-correlation function between a localized and an itinerant spin on a single bond can be expressed in terms of the expectation value of bond operators which can be related to the one-particle Green's function,

$$\sigma \equiv \frac{1}{N}\sum_{i,\alpha}\langle\tau_{i,\alpha}S_{i,\alpha}\rangle = -\frac{3}{4}+\frac{1}{4N}\sum_{k,\alpha}\langle t^\dagger_{k,\alpha}t_{k,\alpha}\rangle = -\frac{3}{4}+\frac{1}{4N}\sum_{k,\alpha}\{[1+2n_B(\Omega_{k,\alpha})]V^2_{k,\alpha}+n_B(\Omega_{k,\alpha})\}. \tag{41}$$

However, the spin-correlation function between localized spins on different bonds or itinerant ones is expressed in terms of two-particle Green's function. First, we calculate the Matsubara representation for dynamical spin susceptibility. Because in this framework Wick's theorem can be applied and we can use a simple analytical continuation for finding the retarded representation and finally obtain the static structure factor. According to the linear-response theory, the diagonal spin susceptibility for localized spins is written by

$$\chi_{\alpha,\alpha}(q,\omega) = \int_{-\infty}^{+\infty}dte^{i\omega t}\langle[S_\alpha(q,t),S_\alpha(-q,0)]\rangle = -\lim_{i\omega_n\to\omega+i0^+}\int_0^\beta d\tau e^{i\omega_n\tau}\langle TS_\alpha(q,\tau)S_\alpha(-q,0)\rangle = \chi_{\alpha,\alpha}(q,i\omega_n\to\omega+i0^+). \tag{42}$$

Fourier transformation of localized spin in terms of bosonic operators is

$$S_\alpha(q) = \frac{1}{2}\left(t_{-q,\alpha}+t^\dagger_{q,\alpha}-i\varepsilon_{\alpha\beta\gamma}\sum_k t^\dagger_{k+q,\beta}t_{k,\gamma}\right). \tag{43}$$

Therefore, spin susceptibility is given by

$$\chi_{\alpha,\alpha}(q,\tau) = -\langle TS_\alpha(q,\tau)S_\alpha(-q,0)\rangle = 2g_{a,\alpha}(q,\tau)+g_{n,\alpha}(q,\tau)+g_{n,\alpha}(q,-\tau)+g^{(2)}(q,\tau), \tag{44}$$

where $g^{(2)}$ is the two-particle Green's function for triplet gas. The combination of Eqs. (42) and (44) gives the following relation for the spin susceptibility

$$\chi_{\alpha,\alpha}(q,i\omega_n) = 2\left(\frac{u_{q,\alpha}v_{q,\alpha}}{i\omega_n-\omega_{q,\alpha}}-\frac{u_{q,\alpha}v_{q,\alpha}}{i\omega_n+\omega_{q,\alpha}}\right)+\frac{u^2_{q,\alpha}}{i\omega_n-\omega_{q,\alpha}}-\frac{v^2_{q,\alpha}}{i\omega_n+\omega_{q,\alpha}}+\frac{v^2_{q,\alpha}}{i\omega_n-\omega_{q,\alpha}}-\frac{u^2_{q,\alpha}}{i\omega_n+\omega_{q,\alpha}}+\int_0^\beta d\tau e^{i\omega_n\tau}g^{(2)}_\alpha(\tau). \tag{45}$$

In Appendix C we have presented the two-particle Green's function for z-component. From the expression in Eq. (45) the static structure factor may be obtained as shown in Appendix C.

VII. NUMERICAL RESULTS

The single-particle excitation should be found from a self-consistent solution of Eqs. (19), (23), (25), (27), and (B1) with the substitutions $u_{k,\alpha}\to\sqrt{Z_{k,\alpha}}U_{k,\alpha}$, $v_{k,\alpha}\to\sqrt{Z_{k,\alpha}}V_{k,\alpha}$, $\omega_{k,\alpha}\to\Omega_{k,\alpha}$ in the corresponding equations. The process is started with an initial guess for $Z_{k,\alpha},\Sigma_{n,\alpha}(k,0),\Sigma_{a,\alpha}(k,0)$ and by using Eq. (19) we find corrected excitation energy and the renormalized Bogoliubov coefficients. This is repeated until convergence is reached. Using the final values for energy gap, renormalization constants and Bogoliubov coefficients, we can calculate the structure factor by Eqs. (41) and (C11) and the internal energy given in Eq. (30).

The specific heat for the 2D isotropic Kondo necklace model versus kT/J and for various $J_\perp/J$ has been plotted in

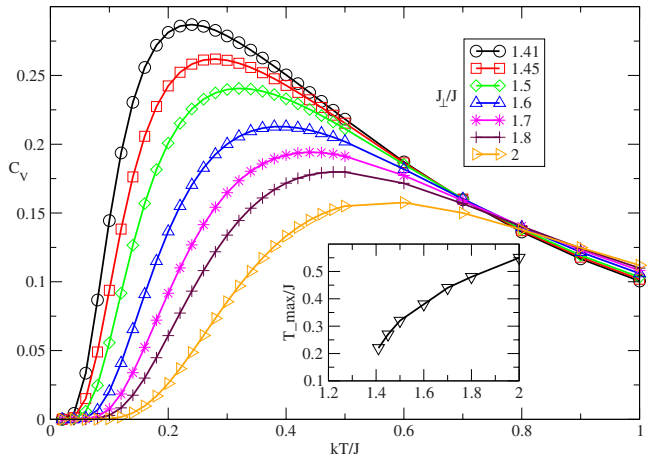

FIG. 1. (Color online) The variation in specific heat C_V versus kT/J for different $J_\perp/J$ in the isotropic Kondo necklace model ($\Delta=1$, $\delta=1$). An increase in $J_\perp/J$ increases the singlet-triplet gap which extends the exponential decay of the specific heat at low temperature. The inset shows the position of the maximum in the specific heat ($T_{\max}/J$) versus $J_\perp/J$ (the same unit of the main figure) which corresponds to the crossover between the Kondo-singlet phase and quantum critical region.

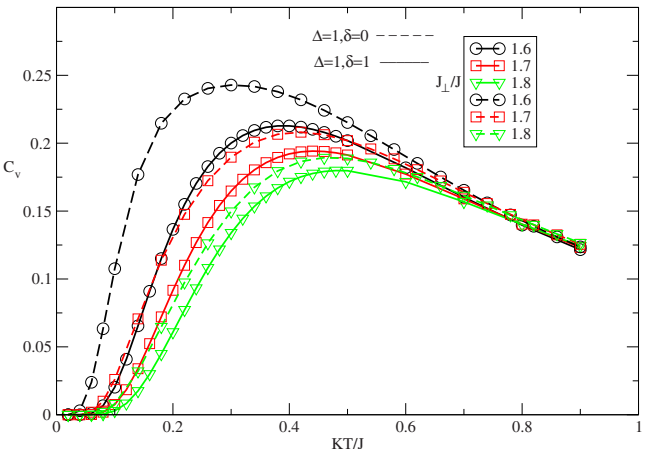

FIG. 2. (Color online) The comparison of specific heat (C_v) in the coupling constants $J_\perp/J=1.6,1.7,1.8$ for two types of anisotropies, $\delta=\Delta=1$ and $\delta=0,\Delta=1$. The dashed lines are related to $\delta=0,\Delta=1$ and solid lines correspond to $\delta=1,\Delta=1$. The reduction of δ increases the peak height of the specific heat and reduces the energy gap.

Fig. 1. Since our approach is based on strong-coupling limit the value of exchange coupling is restricted to $J_\perp/J > (J_\perp/J)_c$ where $(J_\perp/J)_c$ is the quantum critical point at zero temperature. Each curve shows an exponential decay at low temperatures which manifests the presence of a finite-energy gap. Larger values of $J_\perp/J$ show more rapid decay corresponding to larger energy gap. There is also a peak in the specific heat which moves to higher temperature upon increasing $J_\perp/J$. This is similar to the behavior of peak versus the local exchange coupling which has been observed for the Kondo lattice model.[9] The position of the peak ($T_{\_\max}/J$) should correspond to an energy scale which represents the crossover from Kondo-singlet phase to the quantum critical region. We have plotted the value of $T_{\_\max}/J$ versus $J_\perp/J$ as an inset of Fig. 1. The effect of anisotropy has been shown in Fig. 2 where we have plotted the specific heat for ($\Delta=1$, $\delta=1$) and ($\Delta=1$, $\delta=0$). Our data show that the height of the peak in the specific heat increases for $\delta=0$ compared with $\delta=1$. Moreover, the exponential decay at low temperature is reduced for $\delta=0$.

We have also compared the energy gap obtained from the self-consistent numerical solution of the Brueckner equations with the analytical relation given in Eq. (38). Our result is plotted in Fig. 3. It shows that both methods agree for low temperatures and start to deviate for $T/J \simeq 0.3$. This means that for low temperatures $T/J < 0.3$, the single-particle excitations are not affected by the temperature dependence of the self-energy. However, for higher temperatures the latter leads to excitation energies which deviate from those at zero temperature.

The local spin-correlation function (σ) between localized and itinerant spins versus temperature is shown in Fig. 4. The value of σ increases with the local exchange coupling $J_\perp$. On the other hand an increase in temperature reduces the local spin correlations. The value of σ can be used as a criterion for the screening of the localized moments by itinerant spins. In the Kondo lattice model the rapid increase in σ below a particular temperature $T_{\rm FL}$ signifies the onset of Fermi-liquid behavior in the thermodynamic and transport properties. We have also presented the static structure factor $[S(\pi,\pi)]$ for localized spins at the AF wave vector. This function is a measure for the tendency to AF ordering in the localized spins induced by effective interactions via itinerant spins. The static structure factor grows on approaching the quantum critical point which separates Kondo singlet and AF phase. This may be seen from the numerical results for static structure factor which are presented in Fig. 5. We have also calculated σ and $S(\pi,\pi)$ for different anisotropies which show similar qualitative behavior to the isotropic case.

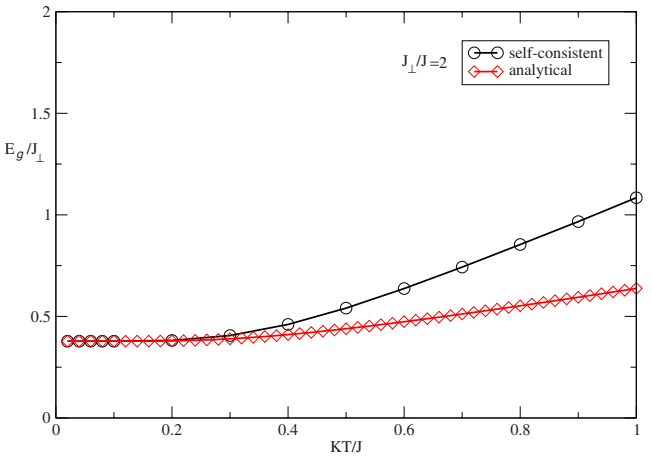

FIG. 3. (Color online) The comparison between self-consistent numerical solution and analytical formula for energy gap $E_g(T)/J_\perp$ versus kT/J and coupling constant $J_\perp/J=2$ in the isotropic Kondo necklace model.

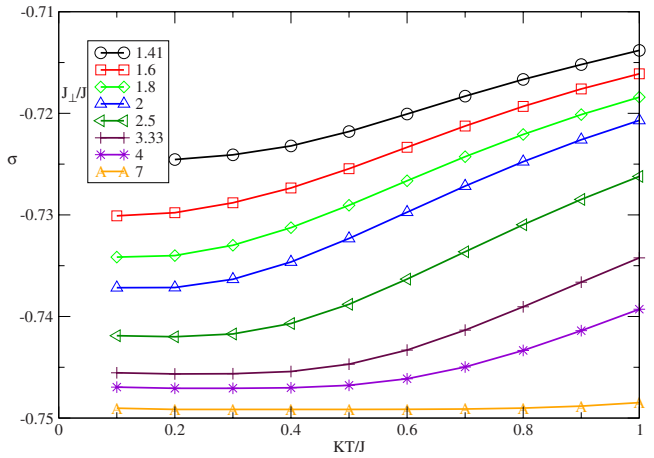

FIG. 4. (Color online) The local spin-correlation function σ versus kT/J and for various amounts for $J_\perp/J$ in the isotropic Kondo necklace model.

VIII. DISCUSSION AND CONCLUSION

We have shown that the hard-core boson approach to the Kondo necklace model can be systematically extended to finite temperatures. The basic assumption used is the low density of triplet excitations. This is naturally justified for moderate temperatures $T \ll J, J_\perp$. Even close to the QCP when the gap closes this assumption is still justified due to the small phase space of the soft triplet mode. We have used self-consistent diagrammatic approach to find nonzero temperature triplet excitation in KNM. Due to the low triplet density we have neglected anomalous Green's function in the scattering amplitude (Γ) for obtaining normal self-energy which is a considerable technical simplification.

The low-temperature behavior of thermodynamic quantities is mostly determined by excitations around the gap threshold for a given T and $J_\perp/J$ in the singlet phase above the QCP value $(J_\perp/J)_c \simeq 1.41$ (in the isotropic case). Therefore the specific heat is expected to show a peak anomaly when the temperature falls below E_g and the triplet excitations become thermally depopulated. The peak appears at a temperature which is fraction of E_g. When the control parameter $J_\perp/J$ increases the singlet becomes more stable and the gap E_g increases. Therefore the maximum in $C(T)$ shifts to higher temperatures. This change in peak position in terms of exchange coupling $J_\perp$ has been found in the KLM with correlated conduction band by cumulant expansion for the partition function.[13] This result is also obtained by finite temperature Lanczos method in the KLM.[9] According to mean-field calculation for finite temperature KNM,[21,22] the low-temperature limit of specific heat in 2D is proportional to $(1/T)e^{-E_g(T)/T}$. The exponential low-temperature decay is clearly present in Fig. 1 but it is not possible to confirm the prefactor from our numerical calculations. We should note that due to finite numerical resolution the gap E_g will not scale exactly to zero at the QCP therefore the exponential decay will always remain at the lowest temperatures.

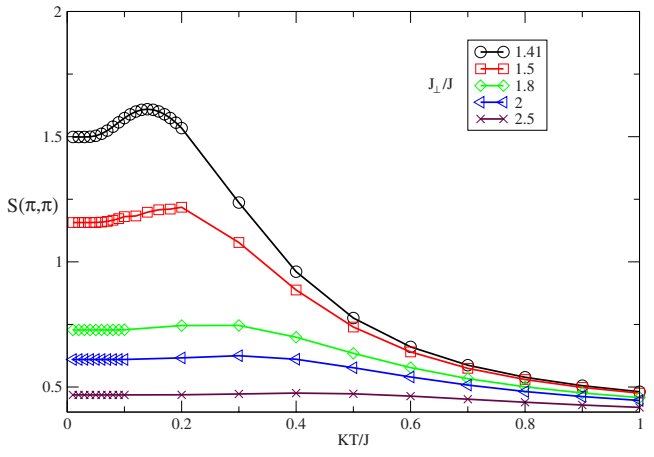

FIG. 5. (Color online) The static structure factor $S(\pi,\pi)$ versus kT/J and for various amounts for $J_\perp/J$ in the isotropic Kondo necklace model.

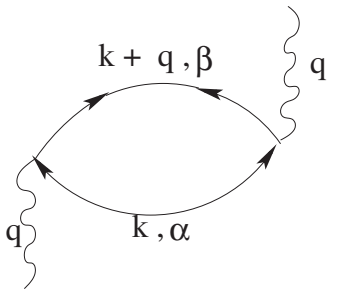

FIG. 6. Random phase approximation part for the first term of the two-particle Green's function in Eq. (C1).

The bond spin-correlation function shown in Fig. 4 is a measure of the Kondo-singlet state. Close to the QCP, it competes with the induced intersite spin interactions which try to break the singlet. Indeed one observes that the value of $|\sigma|$ ($\sigma < 0$) decreases from its maximum 0.75 (corresponding to complete singlet condensation $\bar{s}=1$) in the strong-coupling regime to 0.725 when $T, J_\perp/J$ is close to the QCP. This may seem surprisingly little change. However already on the mean-field level it was noticed that the singlet amplitude close to the QCP is only slightly reduced from $\bar{s}=1$ and this remains so even considerably in the AF regime.[18] This confirms that the starting assumptions of the hard-core boson approach (low density of triplets) is sound. Naturally the local singlet correlations are weakened when temperature is enhanced. This explains the monotonic decrease of $|\sigma|$ in Fig. 4 for all values of $J_\perp/J$.

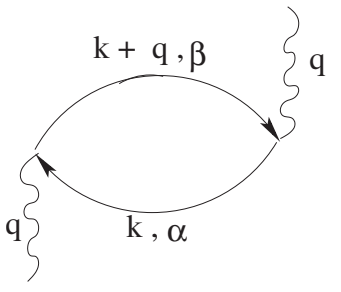

FIG. 7. RPA part for the second term of the two-particle Green's function in Eq. (C1).

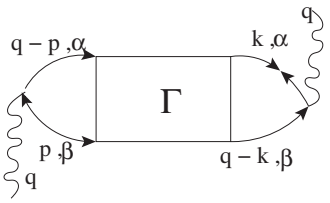

FIG. 8. Vertex correction part for the first term of the two-particle Green's function in Eq. (C1).

The temperature dependence of the static structure factor s(**Q**) at $\mathbf{Q}=(\pi,\pi)$ is quite instructive for the evolution of magnetic correlations in the KNM. The localized spins $\mathbf{S}_i$ in Eq. (1) have no direct interaction. Their interactions are induced via the intersite interaction J of itinerant spins $\boldsymbol{\tau}_i$. The latter however are in singlet bonds with the localized spins due to the local coupling $J_\perp$. Therefore as long as $J_\perp/J$ is large it is hard to polarize the singlets and induce intersite interactions between the $\mathbf{S}_i$ spins. This means that AF correlations between the latter will be weak and only a very broad maximum in $s(\mathbf{Q})$ develops at a temperature corresponding to the typical AF fluctuation energy. As $J_\perp/J$ is reduced the AF intersite correlations are induced more easily, consequently the maximum in $s(\mathbf{Q})$ becomes more pronounced and shifts to lower temperatures. Note however that on approaching the QCP $(J_\perp/J)_c$ from above the characteristic temperature at maximum AF fluctuations does not go to zero. This is because not only the soft mode at **Q** but excitations in the vicinity of the AF wave vector contributes to the AF fluctuations.

In the previous mean-field treatments of the KNM (Refs. 17 and 18) we were able to treat both the Kondo singlet and the AF ordered phase within the bond operator approach. This is possible because even in the AF phase where triplets are condensed $(\bar{t}_\alpha=\langle t_{k,\alpha}\rangle\neq 0)$ one has $\bar{t}_\alpha \ll \bar{s}$ as long as one is not too far in the AF regime. In principle this should also be possible in the hard-core boson approach. But the technical difficulties are considerable and have prevented this analysis for the AF state even at zero temperature.[20] It would however be rewarding to derive both the temperature dependence of the AF structure factor as in Fig. 5 and the AF order parameter for values of $J_\perp/J$ below the QCP.

ACKNOWLEDGMENT

This work was supported in part by the Center of Excellence in Complex Systems and Condensed Matter (www.cscm.ir).

APPENDIX A: MATSUBARA FREQUENCY SUMMATION

In this Appendix, we want to perform the following summation over Matsubara frequencies $Q_m=2m\pi/\beta$ in Eq. (21):

$$S=\frac{1}{\beta}\sum_{Q_m} g_{\alpha\alpha}(Q)g_{\beta\beta}(K-Q). \tag{A1}$$

With the help of Eq. (22), Eq. (A1) may be written as

$$S=\int_{-\infty}^{\infty}\frac{d\omega}{2\pi}R_\alpha(\mathbf{Q},\omega)\int_{-\infty}^{\infty}\frac{d\varepsilon}{2\pi}R_\beta(\mathbf{K}-\mathbf{Q},\varepsilon) \times\frac{1}{\beta}\sum_{Q_m}\frac{1}{iQ_m-\omega}\frac{1}{i\omega_n-iQ_m-\varepsilon}. \tag{A2}$$

The summation may be performed in the usual way by integrating around a contour in complex-frequency plane.[25] The result is

$$\frac{1}{\beta}\sum_{Q_m}\frac{1}{iQ_m-\omega}\frac{1}{i\omega_n-iQ_m-\varepsilon} =-\left[\frac{n_B(\omega)}{i\omega_n-\omega-\varepsilon}-\frac{n_B(-\varepsilon)}{i\omega_n-\varepsilon-\omega}\right]. \tag{A3}$$

According to Eq. (22) the spectral functions in Eq. (A2) are written by

$$\begin{aligned}R_\alpha(\mathbf{Q},\omega)&=-2\,\mathrm{Im}[G_\alpha^{\mathrm{Ret}}(\mathbf{Q},\omega)]\\&=2\pi Z_{\mathbf{Q},\alpha}[U_{\mathbf{Q},\alpha}^2\delta(\omega-\Omega_{\mathbf{Q},\alpha})-V_{\mathbf{Q},\alpha}^2\delta(\omega+\Omega_{\mathbf{Q},\alpha})],\\R_\alpha(\mathbf{K}-\mathbf{Q},\varepsilon)&=-2\,\mathrm{Im}[G_\alpha^{\mathrm{Ret}}(\mathbf{K}-\mathbf{Q},\varepsilon)]\\&=2\pi Z_{\mathbf{K}-\mathbf{Q},\alpha}[U_{\mathbf{K}-\mathbf{Q},\alpha}^2\delta(\varepsilon-\Omega_{\mathbf{K}-\mathbf{Q},\alpha})\\&\quad-V_{\mathbf{K}-\mathbf{Q},\alpha}^2\delta(\varepsilon+\Omega_{\mathbf{K}-\mathbf{Q},\alpha})].\end{aligned} \tag{A4}$$

Then, inserting Eqs. (A4) and (A3) in Eq. (A2) we get Eq. (23) for Γ.

APPENDIX B: SELF-ENERGY DUE TO H_3

In this appendix, we present the normal and anomalous part of self-energy for the x,z components in the second-order perturbation theory with respect to H_3. The final result for self-energies is given by

$$\begin{aligned}\Sigma_{3,x}^n(\mathbf{k},i\omega_n)=&-\frac{J^2}{2N}\sum_q\left[u_{\mathbf{q},y}^2u_{\mathbf{k}+\mathbf{q},z}^2\left(\frac{n_B(\omega_{\mathbf{q},y})-n_B(\omega_{\mathbf{k}+\mathbf{q},z})}{i\omega_n+\omega_{\mathbf{q},y}-\omega_{\mathbf{k}+\mathbf{q},z}}\right)(-\xi_{\mathbf{k}}^2+2\xi_{\mathbf{k}}\xi_{\mathbf{q}}-\xi_{\mathbf{q}}^2)+u_{\mathbf{q},z}^2u_{\mathbf{k}+\mathbf{q},y}^2\right.\\&\left.\times\left(\frac{n_B(\omega_{\mathbf{q},z})-n_B(\omega_{\mathbf{k}+\mathbf{q},y})}{i\omega_n+\omega_{\mathbf{q},z}-\omega_{\mathbf{k}+\mathbf{q},y}}\right)(-\xi_{\mathbf{k}}^2+2\delta\xi_{\mathbf{k}}\xi_{\mathbf{q}}-\delta^2\xi_{\mathbf{q}}^2)\right]-\frac{J^2}{2N}\sum_q\left[u_{\mathbf{q},y}^2u_{\mathbf{k}+\mathbf{q},z}^2\left(\frac{n_B(\omega_{\mathbf{q},y})-n_B(-\omega_{\mathbf{k}+\mathbf{q},z})}{i\omega_n-\omega_{\mathbf{q},y}-\omega_{\mathbf{k}+\mathbf{q},z}}\right)\right.\\&\left.\times(-\delta^2\xi_{\mathbf{k}+\mathbf{q}}^2+\delta\xi_{\mathbf{q}}\xi_{\mathbf{k}+\mathbf{q}})+u_{\mathbf{q},z}^2u_{\mathbf{k}+\mathbf{q},y}^2\left(\frac{n_B(\omega_{\mathbf{q},z})-n_B(-\omega_{\mathbf{k}+\mathbf{q},y})}{i\omega_n-\omega_{\mathbf{q},z}-\omega_{\mathbf{k}+\mathbf{q},y}}\right)(-\xi_{\mathbf{k}+\mathbf{q}}^2+\delta\xi_{\mathbf{q}}\xi_{\mathbf{k}+\mathbf{q}})\right],\end{aligned}$$

$$\Sigma^{a}_{3,x}(\mathbf{k},i\omega_n) = -\frac{J^2}{2N}\sum_{q}\left[u^2_{\mathbf{q},y}u^2_{\mathbf{k+q},z}\left(\frac{n_B(\omega_{\mathbf{q},y})-n_B(\omega_{\mathbf{k+q},z})}{i\omega_n+\omega_{\mathbf{q},y}-\omega_{\mathbf{k+q},z}}\right)(-\xi^2_{\mathbf{k}}+\delta\xi_{\mathbf{k}}\xi_{\mathbf{q+k}}+\xi_{\mathbf{k}}\xi_{\mathbf{q}}-\delta\xi_{\mathbf{q}}\xi_{\mathbf{k+q}})\right.$$
$$\left.+u^2_{\mathbf{k+q},y}\left(\frac{n_B(\Omega_{\mathbf{q},z})-n_B(\omega_{\mathbf{k+q},y})}{i\omega_n+\omega_{\mathbf{q},z}-\omega_{\mathbf{k+q},y}}\right)(-\xi^2_{\mathbf{k}}+\xi_{\mathbf{k}}\xi_{\mathbf{q+k}}+\delta\xi_{\mathbf{k}}\xi_{\mathbf{q}}-\delta\xi_{\mathbf{q}}\xi_{\mathbf{k+q}})\right],$$

$$\Sigma^{n}_{3,z}(\mathbf{k},i\omega_n) = -\frac{J^2}{N}\sum_{q}\left[u^2_{\mathbf{q},x}u^2_{\mathbf{k+q},x}\left(\frac{n_B(\omega_{\mathbf{q},x})-n_B(\omega_{\mathbf{k+q},x})}{i\omega_n+\omega_{\mathbf{q},x}-\omega_{\mathbf{k+q},x}}\right)(-\xi^2_{\mathbf{q}}+2\delta\xi_{\mathbf{k}}\xi_{\mathbf{q}}-\delta^2\xi^2_{\mathbf{k}})\right.$$
$$\left.+u^2_{\mathbf{q},x}u^2_{\mathbf{k+q},x}\left(\frac{n_B(\omega_{\mathbf{q},x})-n_B(-\omega_{\mathbf{k+q},x})}{i\omega_n-\omega_{\mathbf{q},x}-\omega_{\mathbf{k+q},x}}\right)(-\xi^2_{\mathbf{q}}+\xi_{\mathbf{q}}\xi_{\mathbf{q+k}})\right],$$

$$\Sigma^{a}_{3,z}(\mathbf{k},i\omega_n) = -\frac{J^2}{N}\sum_{q}u^2_{\mathbf{q},x}u^2_{\mathbf{k+q},x}\left(\frac{n_B(\omega_{\mathbf{q},x})-n_B(\omega_{\mathbf{k+q},x})}{i\omega_n+\omega_{\mathbf{q},x}-\omega_{\mathbf{k+q},x}}\right)(\delta\xi_{\mathbf{k}}\xi_{\mathbf{q}}-2\xi_{\mathbf{q}}\xi_{\mathbf{k+q}}+\delta\xi_{\mathbf{k}}\xi_{\mathbf{k+q}}-\delta^2\xi^2_{\mathbf{k}}). \tag{B1}$$

In the self-energies of H_3 we only consider terms which are proportional to u^4, because in the low-density limit of the triplet bosons, they are the dominant terms.

APPENDIX C: TWO-PARTICLE GREEN'S FUNCTION $g^{(2)}$ FOR z-COMPONENT SPIN

The two-particle Green's function $g^{(2)}$ for the z-component spin is defined by

$$g^{(2)}_z(q,\tau) = \sum_{k,p}\langle T[t^\dagger_{k+q,x}(\tau)t_{k,y}(\tau)t^\dagger_{p-q,x}(0)t_{p,y}(0)]\rangle$$
$$-\langle T[t^\dagger_{k+q,x}(\tau)t_{k,y}(\tau)t^\dagger_{p-q,y}(0)t_{p,x}(0)]\rangle$$
$$+[x\to y, y\to x]. \tag{C1}$$

Now, we define the off-diagonal one-particle density of triplet bosons

$$\varrho_{xy}(q,\tau) = \sum_k t^\dagger_{k+q,x}t_{k,y}. \tag{C2}$$

Therefore, two-particle Green's function can be expressed by the following relation

$$g^{(2)}_z(q,\tau) = \langle T[\varrho_{xy}(q,\tau)\varrho_{xy}(-q,0)]\rangle - \langle T[\varrho_{xy}(q,\tau)\varrho_{yx}(-q,0)]\rangle$$
$$+[x\to y, y\to x]. \tag{C3}$$

To consider the correction effects on the loop of two-particle Green's function we should add two parts. (1) We can separately consider the correction in the interacting terms including H_U for each of the lines of the bubble which are represented in Figs. 6 and 7. These are similar to random-phase approximation (RPA) (Ref. 24) for the charge response function in the electron gas. (2) Considering vertex corrections according to Figs. 8 and 9 for each of Figs. 6 and 7. After summation over Matsubara frequencies the RPA part for the first term in Eq. (C1) which is represented in the Fig. 6 may be written as

$$\frac{1}{\beta}\sum_{k,m} g_{a,\alpha}(k-q,i\omega_n-ik_m)g_{a,\beta}(k,ik_m)$$
$$= -\frac{1}{N}\sum_k Z_{k-q,\alpha}Z_{k,\beta}U_{k-q,\alpha}V_{k-q,\alpha}U_{k,\beta}V_{k,\beta}$$
$$\times\left(\frac{n_B(\Omega_{k,\beta})-n_B(-\Omega_{k-q,\alpha})}{i\omega_n-\Omega_{k-q,\alpha}-\Omega_{k,\beta}}-\frac{n_B(-\Omega_{k,\beta})-n_B(-\Omega_{k-q,\alpha})}{i\omega_n-\Omega_{k-q,\alpha}+\Omega_{k,\beta}}\right.$$
$$\left.-\frac{n_B(\Omega_{k,\beta})-n_B(\Omega_{k-q,\alpha})}{i\omega_n+\Omega_{k-q,\alpha}-\Omega_{k,\beta}}+\frac{n_B(-\Omega_{k,\beta})-n_B(\Omega_{k-q,\alpha})}{i\omega_n+\Omega_{k-q,\alpha}+\Omega_{k,\beta}}\right). \tag{C4}$$

Furthermore, RPA part for the second term of Eq. (C1) is represented in Fig. 7 and is given by

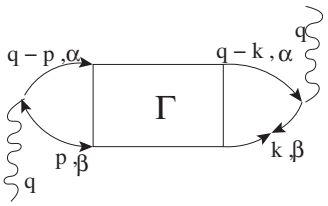

FIG. 9. Vertex correction part for the second term of the two-particle Green's function in Eq. (C1).

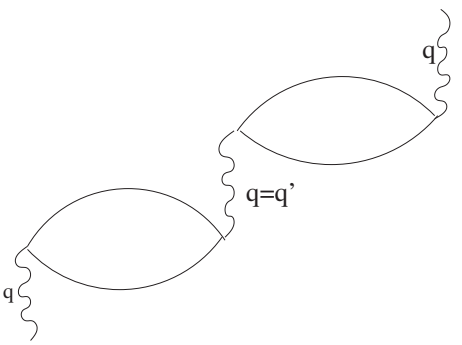

FIG. 10. Two closed loops which have no contribution for the two-particle Green's function (C3).

$$\frac{1}{\beta}\sum_{k,m} g_{n,\alpha}(k+q,i\omega_n+ik_m)g_{n,\beta}(k,ik_m)$$
$$=\frac{1}{N}\sum_{k} Z_{k+q,\alpha}Z_{k,\beta}\Bigg(U^2_{k+q,\alpha}U^2_{k,\beta}\frac{n_B(\Omega_{k,\beta})-n_B(\Omega_{k+q,\alpha})}{i\omega_n-\Omega_{k+q,\alpha}+\Omega_{k,\beta}}$$
$$+V^2_{k+q,\alpha}U^2_{k,\beta}\frac{n_B(\Omega_{k,\beta})-n_B(-\Omega_{k+q,\alpha})}{i\omega_n+\Omega_{k+q,\alpha}+\Omega_{k,\beta}}$$
$$+U^2_{k+q,\alpha}V^2_{k,\beta}\frac{n_B(-\Omega_{k,\beta})-n_B(\Omega_{k+q,\alpha})}{i\omega_n-\Omega_{k-q,\alpha}-\Omega_{k,\beta}}$$
$$-V^2_{k+q,\alpha}V^2_{k,\beta}\frac{n_B(-\Omega_{k,\beta})-n_B(-\Omega_{k-q,\alpha})}{i\omega_n+\Omega_{k-q,\alpha}-\Omega_{k,\beta}}\Bigg). \quad \text{(C5)}$$

The vertex correction for the first term in the Eq. (C1) is shown in Fig. 8 and it is written as

$$\Bigg(-\frac{1}{\beta}\sum_{k,m} g_{n,\alpha}(-k+q,i\omega_n-ik_m)g_{a,\beta}(k,ik_m)\Bigg)^2\Gamma^{\alpha\beta,\alpha\beta}(q,i\omega_n)$$
$$=\Bigg[\frac{1}{N}\sum_{k} Z_{k+q,\alpha}Z_{k,\beta}\Bigg(-U^2_{k+q,\alpha}U_{k,\beta}V_{k,\beta}\frac{n_B(\Omega_{k,\beta})-n_B(-\Omega_{k+q,\alpha})}{i\omega_n-\Omega_{k+q,\alpha}-\Omega_{k,\beta}}+U^2_{k+q,\alpha}U_{k,\beta}V_{k,\beta}\frac{n_B(\Omega_{k,\beta})-n_B(\Omega_{k+q,\alpha})}{i\omega_n+\Omega_{k+q,\alpha}-\Omega_{k,\beta}}$$
$$-U^2_{k+q,\alpha}U_{k,\beta}V_{k,\beta}\frac{n_B(-\Omega_{k,\beta})-n_B(-\Omega_{k+q,\alpha})}{i\omega_n-\Omega_{k-q,\alpha}+\Omega_{k,\beta}}-V^2_{k+q,\alpha}U_{k,\beta}V_{k,\beta}\frac{n_B(-\Omega_{k,\beta})-n_B(\Omega_{k-q,\alpha})}{i\omega_n+\Omega_{k-q,\alpha}+\Omega_{k,\beta}}\Bigg)\Bigg]^2\Gamma^{\alpha\beta,\alpha\beta}(q,i\omega_n). \quad \text{(C6)}$$

The vertex correction for the second term in Eq. (C1) is represented in Fig. 9 and is as follows:

$$\Bigg(-\frac{1}{\beta}\Bigg)^2\sum_{k,m,p,l} g_{n,\alpha}(-p+q,i\omega_n-ip_l)g_{a,\alpha}(k,ik_m)g_{n,\beta}$$
$$\times(-k+q,i\omega_n-ik_m)g_{a,\beta}(p,ip_l)\Gamma^{\alpha\beta,\alpha\beta}(q,i\omega_n). \quad \text{(C7)}$$

Figure 10 has two closed loops that represent the first-order correction for the two-particle Green's function, connected by an interaction line (U_q). This diagram is zero because the first-order correction induced to H_U for the spin susceptibility is written by

$$\langle T[\varrho_{xy}(q,\tau)\varrho_{xy}(-q,0)]\rangle$$
$$=\sum_{k,p,k_1,p_1,q_1,\alpha,\beta}\int d\tau_1\langle Tt^\dagger_{k+q,x}(\tau)t_{k,y}(\tau)U_{q_1}t^\dagger_{k_1+q_1,\alpha}$$
$$\times(\tau_1)t^\dagger_{p_1-q_1,\beta}(\tau_1)t_{p_1,\beta}(\tau_1)t_{k_1,\alpha}(\tau_1)t^\dagger_{p-q,x}(0)t_{p,y}(0)\rangle. \quad \text{(C8)}$$

To obtain the Feynman diagram in Fig. 10, we should consider the contraction with $q_1=q$. This constraint requires that the term $t^\dagger_{p-q,x}(0)t_{p,y}(0)$ is contracted by $t^\dagger_{p_1-q_1,\beta}(\tau_1)t_{p_1,\beta}(\tau_1)$ therefore $\beta=x=y$ and this is a contradiction. However, we note that the vertex correction in Eqs. (C6) and (C7) for the z component of susceptibility are exactly the same and vanish in Eq. (C1).

The dynamical structure factor is defined by

$$s_\alpha(q,\omega)=-2\ \mathrm{Im}\ \chi^{\mathrm{Ret}}(q,\omega)=-2\ \mathrm{Im}\ \chi(q,i\omega_n\to\omega+i0^+). \quad \text{(C9)}$$

It is proportional to the contribution of localized spins in the inelastic neutron differential cross section. For each q the dynamical structure factor has peaks at certain energies which represent collective excitations for bosonic triplet gas which correspond to the spin excitations of the original model. The static structure factor is defined by

$$s_\alpha(q)=\langle S_\alpha(q)S_\alpha(-q)\rangle=\chi^{\alpha\alpha}(q,0)$$
$$=-\frac{1}{\beta}\sum_n\frac{1}{2\pi}\int_{-\infty}^{\infty}d\omega\frac{-2\ \mathrm{Im}\ \chi_{\alpha\alpha}(q,i\omega_n\to\omega+i0^+)}{i\omega_n-\omega}$$
$$=-\int_{-\infty}^{+\infty}d\omega\frac{n_B(\omega)}{\pi}\mathrm{Im}\ \chi_{\alpha\alpha}(q,i\omega_n\to\omega+i0^+). \quad \text{(C10)}$$

Combining Eqs. (45) and (C10) the z component of the structure factor is given by

$$s_z(q)=Z_{q,z}[2U_{q,z}V_{q,z}+U^2_{q,z}+V^2_{q,z}][n_B(\Omega_{q,z})-n_B(-\Omega_{q,z})]$$
$$-\frac{2}{N}\sum_k U_{k,z}U_{k+q,z}V_{k+q,z}V_{k,z}\{[n_B(\Omega_{k,z})-n_B(-\Omega_{k+q,z})]n_B(\Omega_{k,z}+\Omega_{k+q,z})-[n_B(-\Omega_{k,z})-n_B(-\Omega_{k+q,z})]n_B(-\Omega_{k,z}+\Omega_{k+q,z})$$
$$-[n_B(\Omega_{k,z})-n_B(\Omega_{k+q,z})]n_B(\Omega_{k,z}-\Omega_{k+q,z})+[n_B(-\Omega_{k,z})-n_B(\Omega_{k+q,z})]n_B(-\Omega_{k,z}-\Omega_{k+q,z})\}$$

$$-\frac{2}{N}\sum_{k} Z_{k,z}Z_{k+q,z}\{U_{k,z}^2U_{k+q,z}^2[n_B(\Omega_{k,z})-n_B(-\Omega_{k+q,z})]n_B(\Omega_{k,z}+\Omega_{k+q,z})$$
$$+U_{k,z}^2V_{k+q,z}^2[n_B(-\Omega_{k,z})-n_B(-\Omega_{k+q,z})]n_B(-\Omega_{k,z}+\Omega_{k+q,z})+U_{k+q,z}^2V_{k,z}^2[n_B(\Omega_{k,z})-n_B(\Omega_{k+q,z})]n_B(\Omega_{k,z}-\Omega_{k+q,z})$$
$$-V_{k+q,z}^2V_{k,z}^2[n_B(-\Omega_{k,z})-n_B(\Omega_{k+q,z})]n_B(-\Omega_{k,z}-\Omega_{k+q,z})\}. \quad \text{(C11)}$$

*langari@sharif.edu; http://spin.cscm.ir

[1] P. Gegenwart, Q. Si, and F. Steglich, Nat. Phys. **4**, 186 (2008).
[2] Q. Si, S. Rabello, K. Ingersent and J. L. Smith, Nature **413**, 804 (2001).
[3] A. C. Hewson, *The Kondo Problem to Heavy Fermions* (Cambridge University Press, New York, 1993).
[4] M. Vojta, Rep. Prog. Phys. **66**, 2069 (2003).
[5] J. A. Hertz, Phys. Rev. B **14**, 1165 (1976).
[6] A. J. Millis, Phys. Rev. B **48**, 7183 (1993).
[7] F. F. Assaad, Phys. Rev. Lett. **83**, 796 (1999); S. Capponi and F. F. Assaad, Phys. Rev. B **63**, 155114 (2001).
[8] N. Shibata, B. Ammon, M. Sigrist, and K. Ueda, J. Phys. Soc. Jpn. **67**, 1086 (1998); N. Shibata, K. Ueda, J. Phys.: Condens. Matter **11**, R1 (1999).
[9] I. Zerec, B. Schmidt, and P. Thalmeier, Phys. Rev. B **73**, 245108 (2006).
[10] I. Zerec, B. Schmidt, and P. Thalmeier, Physica B **378-380**, 702 (2006).
[11] S. Doniach, Physica B & C **91**, 231 (1977).
[12] T. Schork, S. Blawid, and J. I. Igarashi, Phys. Rev. B **59**, 9888 (1999).
[13] Q. Gu, Phys. Rev. B **66**, 052404 (2002).
[14] Ch. Brünger and F. F. Assaad, Phys. Rev. B **74**, 205107 (2006).
[15] A. V. Chubukov, JETP Lett. **49**, 129 (1989).
[16] S. Sachdev and R. N. Bhatt, Phys. Rev. B **41**, 9323 (1990).
[17] A. Langari and P. Thalmeier, Phys. Rev. B **74**, 024431 (2006).
[18] P. Thalmeier and A. Langari, Phys. Rev. B **75**, 174426 (2007).
[19] S. Mahmoudian and A. Langari, Phys. Rev. B **77**, 024420 (2008).
[20] H. Rezania, A. Langari, and P. Thalmeier, Phys. Rev. B **77**, 094438 (2008).
[21] D. Reyes, M. A. Continentino, and H.-T. Wang, arXiv:0801.2792 (unpublished).
[22] D. Reyes and M. A. Continentino, Phys. Rev. B **76**, 075114 (2007).
[23] P. V. Shevchenko, A. W. Sandvik, and O. P. Sushkov, Phys. Rev. B **61**, 3475 (2000).
[24] G. D. Mahan, *Many Particle Physics* (Kluwer Academics/Plenum Publishers, New York, 2000).
[25] A. L. Fetter and J. D. Walecka, *Quantum Theory of Many-Particle Systems* (MacGraw-Hill, New York, 1971).
[26] V. N. Kotov, O. Sushkov, Zheng Weihong, and J. Oitmaa, Phys. Rev. Lett. **80**, 5790 (1998).
[27] Zheng Weihong, Phys. Rev. B **55**, 12267 (1997).
[28] K. Hida, J. Phys. Soc. Jpn. **61**, 1013 (1992).